Jestr

Journal of Engineering Science and Technology Review 15 (2) (2022) 22 - 31

JOURNAL OF
Engineering Science and Technology Review

Research Article

www.jestr.org

Experimental Study on Axial Compression Behavior of Semi-precast Composite Shear Wall

Xiaoruan Song[1], Chenglin Huang[2], Shili Luo[1,*], Song Huang[1] and Zhichao Zhang[1]

[1]*North China University of Technology, Beijing 100144, China*
[2]*China United Engineering Corporation Limited. No. 1060 Bin'an Rd., Hangzhou 310052, China*

Received 15 January 2022; Accepted 2 May 2022

Abstract

To overcome the complex manufacturing process and large amount of steel used in the precast concrete plate with lattice reinforcement, a new-type semi-precast composite shear wall structure was proposed. Through the axial compression test on 7 shear wall specimens, the effects of the interface connection modes, the ribs, studs and CFRP (carbon fiber reinforced-polymer) shear connectors on the axial compression performance of the composite shear wall were studied. Compared with full cast-in-place shear wall, the failure state, mechanical performance, deformation and bearing capacity of the new proposed specimens under axial load were analyzed. Results show that the failure modes of specimens are mainly divided into two types: the superposition surface failure and wall compression failure. Setting stud or CFRP shear connectors at the interface can effectively improve the bonding performance between the precast cement plate and wall core concrete, so the axial compression bearing capacity of composite shear wall is significantly improved. The deformation of the composite shear wall specimens is similar to that of the full cast-in-place shear wall. The steel and concrete strains of the specimens with the CFRP shear connectors at the interface can change synchronously, showing a better cooperative stress performance. The theoretical values obtained from the calculation of the axial compression bearing capacity are in good agreement with the experimental values. The conclusions obtained in this study provide a reference for design and application of the new composite shear wall.

Keywords: Composite shear wall, Axial compression, Interface connection mode, Stud, shear connectors

1. Introduction

Precast concrete structures have become a popular choice in the existing structure form because of its fast construction speed on site, energy saving and emission reduction. The structures also save conventional templates and do not require extra support; therefore, the advantages in terms of saving the manpower and materials should also be noted. The precast concrete shear wall structure system has the advantages of large lateral stiffness, high bearing capacity and regular indoor space. It is an important structural system researched and developed in China for the past years, which is in line with the strategic goal of the sustainable development of buildings. Precast concrete shear wall structure system can be divided into two types, including the full precast shear wall structure system and composite shear wall structure system. Particularly, the overall performance of the full prefabricated shear wall structure system is slightly poor. Since the horizontal joint and the connection structure of the related nodes between the prefabricated walls are complex, and the construction is difficult. Hence, it is difficult to achieve the same behaviour as the cast-in-place concrete structure. Therefore, the composite shear wall structure system has gained more attention in this field [1-3].

The composite shear wall structure system shows both the advantages of the cast-in-place concrete structure and precast concrete structure with the improved performance under loading. It allows certain installation errors in construction, reduces the assembly difficulty of components [4,5]. For the existing composite shear wall structures, the bonding performance of the joint surface between the precast concrete plate and the wall core concrete is enhanced by setting lattice reinforcement in the precast concrete plate. However, the fabrication process of the precast concrete plate with lattice reinforcement is complex and the amount of steel used is large. When this kind of composite shear wall structure is applied to high-rise buildings, the lattice reinforced composite structure exhibits the inconvenient construction due to the thick and heavy plates.

Therefore, it is necessary to improve the bonding performance of composite shear wall, simplify the manufacturing process of the precast plate and reduce its weight. A new-type composite shear wall structure system was proposed in this study, and its axial compression performance was studied to provide reference for the design and engineering application of this composite shear wall.

2. State of the art

So far, many scholars have performed a lot of research on the performance of the composite shear wall. Benayoune et al. conducted compression tests under the axial and eccentric loads on 6 composite shear wall specimens with lattice reinforcement. They found that the overall performance of the composite shear wall was good, and the precast concrete plates on both sides could work together. With the increase of the slenderness ratio, the bearing capacity increases nonlinearly [6,7]. Frankl et al. prepared six composite shear

*E-mail address: 934919512@qq.com
ISSN: 1791-2377
doi:10.25103/jestr.152.04

walls with prestressed steel bars and placed the samples under the axial and reversed cyclic lateral load. They found that the stiffness and deformation of the composite shear walls were closely related to the form of shear connectors. They also found that the CFRP (carbon fiber reinforced-polymer) shear connectors could provide effective shear transfer [8]. Tomlinson et al. conducted an experimental study on the out-of-plane bending performance of the composite shear walls, and found that the bearing capacity of specimens increased with the increase of the reinforcement ratio of GFRP shear connectors [9]. Bei et al. conducted reverse cyclic loading tests on four composite shear wall specimens with bolted connections with different types of steel plates. They found that the bolted steel plate with horizontal slots could improve the ductility and energy dissipation of the precast shear wall joints [10]. Mohamad et al. tested 6 pieces of prefabricated lightweight foam concrete composite wall panels under the action of axial load. They found that the axial compressive bearing capacity of wallboard was related to the strength of the bottom of the panel and the lightweight foam concrete. During the loading process, the wall panels on both sides worked well in the same direction [11,12].

In China, some scholars focused on the overall performance, seismic performance and the interface connection of composite shear wall structure. Ye et al. conducted pseudo-static tests on composite shear wall specimens with different axial compression ratios [13]. Wang et al. proposed a composite shear wall with concealed bracings and carried out pseudo-static tests. They found that the steel plate support could effectively improve the bearing capacity and ductility of the composite shear wall [14]. Li et al. carried out uniaxial tensile test on 60 indirect lap specimens with vertical distribution steel bars in sandwich insulation composite shear walls with different parameters. They found that increasing the strength of concrete could improve the bearing capacity of specimens, and that a shorter lap length of the steel bars showed better improved capacity [15]. Chu et al. proposed a composite shear wall with no lattice reinforcement. However, the precast concrete plates were treated with key slots or rough surfaces. They found that the interface treatment methods could effectively connect the precast concrete plate and the cast-in-place concrete. The seismic performance was improved and the key groove connection performance was better than the rough surface connection [16].

The bonding performance between the precast concrete plate and the cast-in-place concrete is a key factor affecting the performance of composite shear wall structure. Setting lattice reinforcement on precast concrete plate enhances the bonding performance and maintains a good integrity. However, the fabrication process of this kind of precast concrete plate with lattice reinforcement is complex and the weight of the plate is too large, which limits the engineering application in the industry.

In view of the shortcomings of the existing research, we proposed a new-type semi-prefabricated composite shear wall structure system with fiber reinforced composite cement plate [17-21]. Six semi-prefabricated composite specimens and one full cast-in-place specimen were prepared and subjected to axial compression tests. The failure process, mechanical performance, deformation and bearing capacity of each specimen were recorded and analyzed. The influence of interface connection modes including ribs, studs and CFRP shear connectors on the axial compression performance of composite shear wall were studied. The experimental results of this work should provide basis for the design and application of the new-type composite shear wall.

The rest of this study is organized as follows. Section 3 introduces the axial compression test scheme of composite shear wall. Section 4 analyzes the axial compression test results of composite shear walls, and finally, the conclusions are summarized in Section 5.

3. Methodology

3.1 Specimen preparation

Seven shear wall specimens were designed in this study, including one full cast-in-place reinforced concrete shear wall (CSW1), three composite shear walls (CSW2-4) and three thermal insulation composite shear walls (CSW5-7). The precast basalt fiber reinforced composite cement plates with a thickness of 10 mm were placed on both sides with a 100 mm thick concrete casted in the middle (CSW2-4), and the thickness of the other three thermal insulation composite shear wall specimens (CSW5-7) was 170 mm. One side of the thermal insulation composite concrete shear wall specimen was 50 mm precast cement thermal insulation composite plate and one side was the 10 mm thick precast basalt fiber reinforced composite cement plate. The middle core concrete was 110 mm thick. The precast composite cement plate and the composite insulation plate on both sides can be used as wall formwork during construction. According to the Chinese Code for Design of Concrete Structures (GB50010-2010), the longitudinal reinforcement bars of all shear wall specimens is given as 10B8 and the transverse reinforcement bars is determined as A6@105. The main design parameters and interface connection modes of the specimens are shown in Table 1. The size and reinforcement of each specimen are shown in Fig. 1.

The schematic diagram of the precast basalt fiber reinforced composite cement plate is shown in Fig. 2. The cement, coal fly ash, expanded perlite, sand, water reducing agent and the coupling agent was mixed with a proportion of 1: 0.25 : 0.015 : 0.15 : 0.007 : 0.015. A thin layer of basalt fiber grid cloth was placed near the upper and lower surface of the cement plate. The specification of basalt fiber grid cloth was 160 g/m^2, the mesh size was 5 mm × 5 mm and the thickness was 0.65 mm. The precast cement insulation composite plate was a basalt fiber reinforced cement plate poured on the slotted rigid polyurethane foaming plastics insulation plate, as shown in Fig. 3. The interface connection of the two types of composite shear wall specimens utilized the ribs, studs and CFRP shear connectors. The precast concrete plate with ribs is shown in Fig. 4.

Table 1. Main design parameters of specimens.

Test specimen number	Wall types	Width (mm)	Thickness (mm)	Interface connection mode
CSW1	Full cast-in-place concrete shear wall	500	120	——
CSW2	Composite shear wall	500	120	Rib
CSW3	Composite shear wall	500	120	Rib and stud
CSW4	Composite shear wall	500	120	Rib and CFRP shear connector
CSW5	Thermal insulation composite shear wall	500	170	Rib

CSW6	Thermal insulation composite shear wall	500	170	Rib and stud
CSW7	Thermal insulation composite shear wall	500	170	Rib and CFRP shear connector

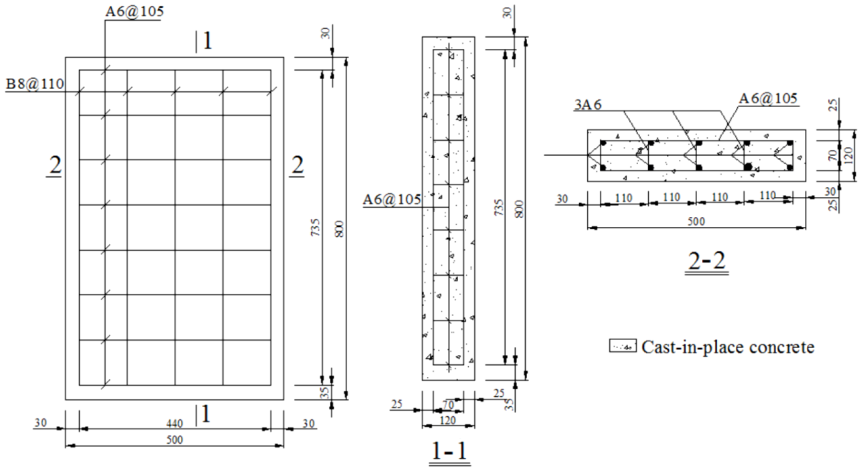

(a) Specimen CSW1

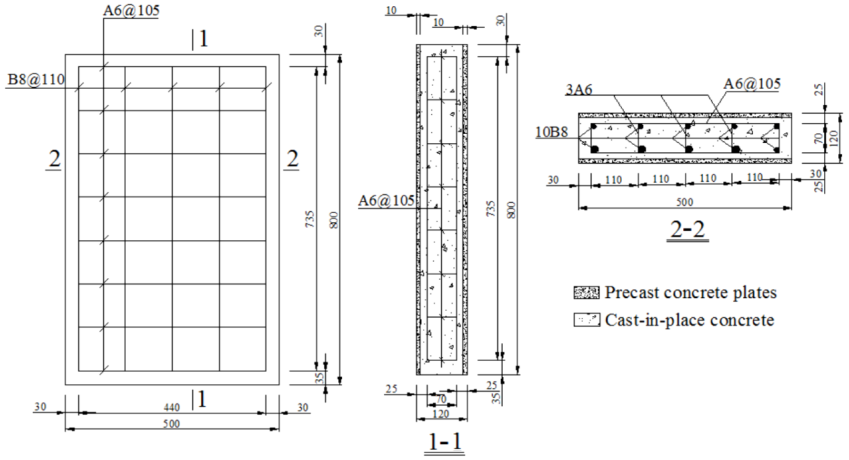

(b) Specimen CSW2-4

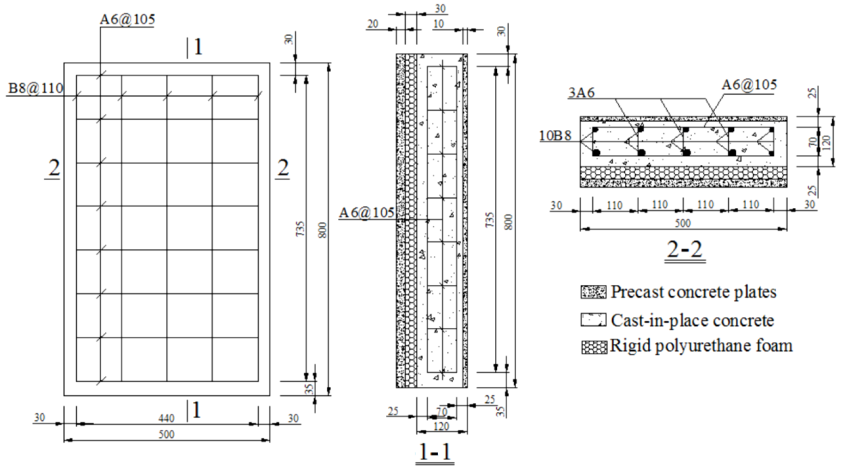

(c) Specimen CSW5-7

Fig. 1. Size and reinforcement of each specimen.

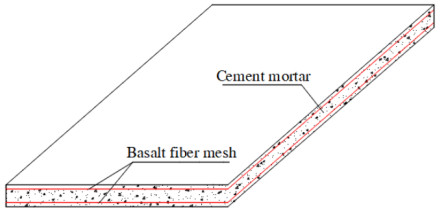

Fig. 2. Schematic diagram of precast composite cement plate.

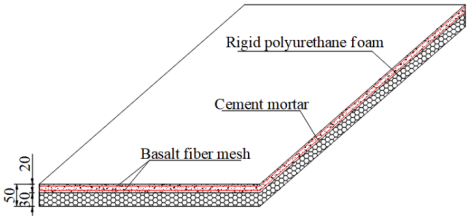

Fig. 3. Schematic diagram of precast cement insulation composite plate.

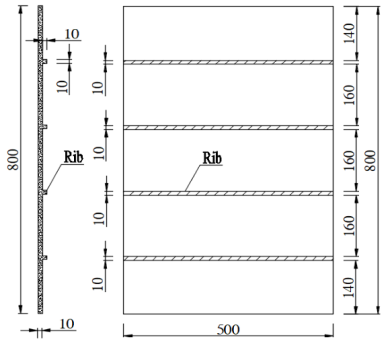

Fig. 4. Schematic diagram of ribbed precast cement plate.

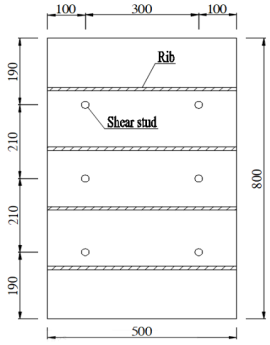

Fig. 5. Position layout of studs.

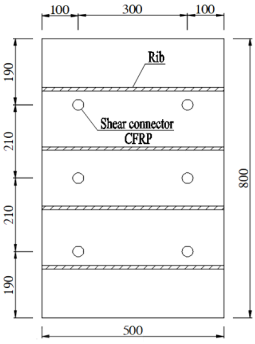

Fig. 6. CFRP shear connectors.

In the process of making specimens, 150 mm × 150 mm × 150 mm concrete standard cube test block and 150 mm × 150 mm × 300 mm concrete prism test block were reserved for precast cement plate and cast-in-place wall core concrete. After 28 d of natural curing under the same conditions with shear wall specimens, the concrete material properties were tested respectively. The mechanical properties of concrete materials are shown in Table 2. In the same batch of steel bar materials, each type of size of steel bars was reserved three specimens of 450 mm length, the same batch of carbon fiber bars were reserved three specimens of 450 mm length. The mechanical properties of steel bars and carbon fiber bars are shown in Table 3.

3.2 Test equipment and loading system

The vertical axial force was applied by the electro-hydraulic servo pressure testing machine, and the force control monotonic loading scheme was adopted. In order to ensure the smooth loading surface, the mortar layer was laid on the bottom and top of the specimen, and the specimen was accurately aligned to ensure the axial compression of the specimen. The loading device is shown in Fig. 7.

During the test, preload first, and then unload back to zero. When formal loading was carried out, the graded uniform loading method was adopted. Firstly, the load increment of each stage was controlled to be 100 kN. When cracks occur in the specimen, the load increment of each stage was changed to 50 kN, and the load of each stage was stable for 3 min. According to this loading system, the specimen was loaded until failure.

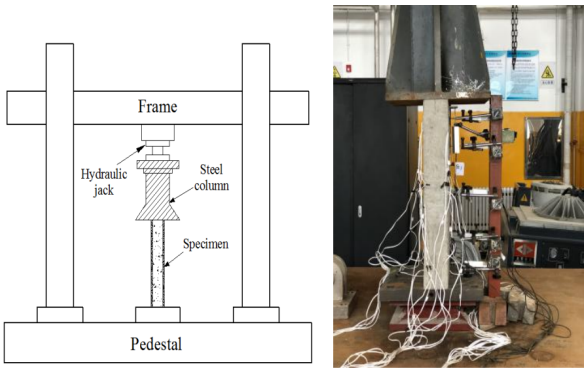

(a) Schematic (b) Photograph

Fig. 7. Loading device.

Table 2. Mechanical parameters of the standard concrete samples.

Concrete type	Cube crushing strength (MPa)	Axial compressive strength (MPa)	Elastic modulus (GPa)
Precast cement plate	47.83	30.13	32.8
Wall core concrete	38.24	26.21	30.1

Table 3. Mechanical properties of steel bars and carbon fiber bars.

Model	Diameter (mm)	Yield strength (MPa)	Tensile strength (MPa)	Elastic modulus (GPa)
Steel HPB300	6	297	408	208
Steel HRB335	8	332	446	201
Carbon fiber tendon	10	—	905	126

3.3 Test procedures

For measuring the vertical and lateral displacements of the composite shear wall specimens during loading, a total of six displacement meters were arranged, of which five meters labeled LD1- LD5 were arranged on the central line of the wall to measure the lateral displacement of the specimen along the height direction of the wall, and the last meter VD6 was set on the top of the central line of the wall to measure the vertical displacement. The displacement meter arrangement is shown in Fig. 8(a).

To measure the strain of the longitudinal reinforcement along different heights, strain gauges were placed on the two columns of the longitudinal reinforcement in the middle of the reinforcement network. The measuring points were 60 mm from the top surface, 60, 200, 400, 600, 740 mm from the bottom surface of the sample (see Fig. 8(b)). Another five strain measuring points were arranged on the center line of the precast formwork on both sides to measure the longitudinal strain of concrete (precast cement plate). The measuring points were also located at 60, 200, 400, 600, 740 mm from the top surface, respectively. The strain gauge layout of steel and concrete is shown in Figs. 8(b) and 8(c). During the test, the load, displacement and strain were recorded by the IMP automatic data acquisition system.

4. Results analysis and discussion

4.1 Test phenomenon and failure mode

According to the experimental phenomena of composite shear wall under axial load, its failure modes were mainly divided into two types: the bonding surface failure and the axial compression failure. Among them, the specimen CSW2 with ribs at the interface was damaged by the superposition plane. At the beginning of loading, there was

no obvious failure shown on the surface of the specimen CSW2. When the load was added to 500 kN, cracks began to appear at the joint between the wall core concrete and the precast cement plate. With the continuous increase of the load, the cracks at the joint extended and expanded. When the load was 1000 kN, part of the precast cement plate on one side of the specimen and the wall core concrete were sloughing. When the load was added to about 1230 kN, however, the precast cement plates on both sides of the specimen were completely separated and the loading stopped. The failure state of specimen CSW2 is shown in Fig. 9. The precast concrete plate bent at the 2/5 height from the bottom, and there was a horizontal crack of 25 cm long at the bending position. However, due to the existence of fiber cloth, the precast concrete plate still maintained a good integrity. The ribs on both sides of the precast concrete plate were completely separated from the core concrete, and there was no obvious damage seen on the concrete.

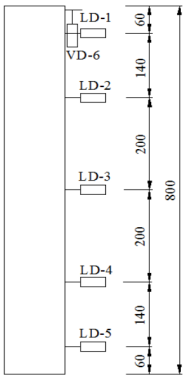

(a) Layout of displacement meters

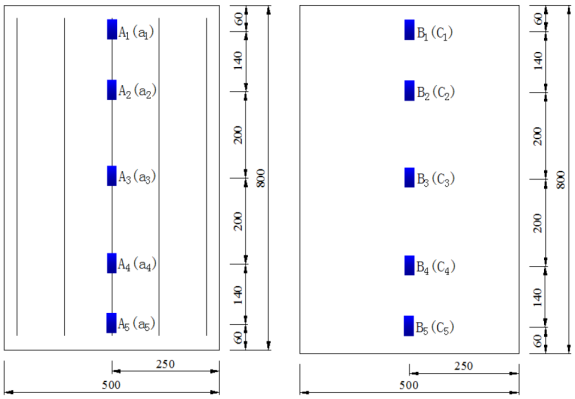

(b) Layout of steel strain gauges (c) Layout of concrete strain gauges

Fig. 8. Layout of measuring points.

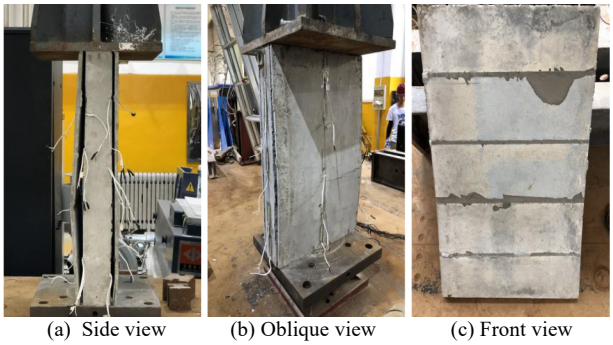

(a) Side view (b) Oblique view (c) Front view

Fig. 9. Failure characteristics of CSW2 specimen.

The failure states of the composite specimens with ribs, studs or shear connectors at the interface and the full cast-in-place specimen are shown in Fig. 10.

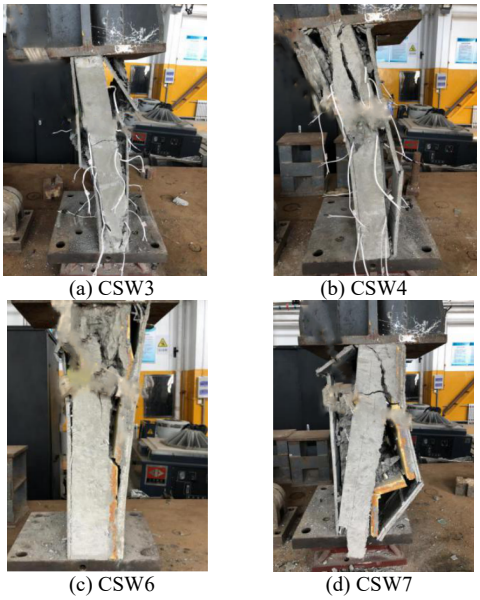

(a) CSW3 (b) CSW4

(c) CSW6 (d) CSW7

Fig. 10. Axial compression failure.

The failure process of the composite shear wall with axial compression failure has the basic and similar characteristics. In the early stage of loading, the precast concrete plates on both sides of the specimen were well bonded with the wall core concrete. With the increase of the load, the cracks began to appear at the joint between the precast concrete plates and the wall core concrete. The cracks then started to extend and expand. At the end of the test, the specimen was crushed and accompanied by a huge noise. When the specimen was crushed, the wall core concrete and the precast concrete plates were still well bonded at most parts. By observing the final failure states of the specimens, it can be seen that the wall core concrete was seriously damaged, with a large number of fragments. The steel mesh in the wall core concrete was also seriously bending. On the other hand, the damage of the precast cement plate and precast cement insulation composite plate were not as serious as that of wall core concrete though was a broken phenomenon in the body of the board. However, the fiber grid cloth played an important role in restricting wall core concrete and also maintaining the integrity of the precast cement board and precast cement insulation composite board. Compared with the failure states of the cast-in-place reinforced concrete specimen CSW1, when the specimen CSW1 was crushed, the concrete fragments fall seriously, and the composite shear wall still maintained a good integrity when the prefabricated templates on both sides were crushed, so that the concrete fragments of the wall core would not fall outside the wall. The comparison analysis is shown in Fig. 11.

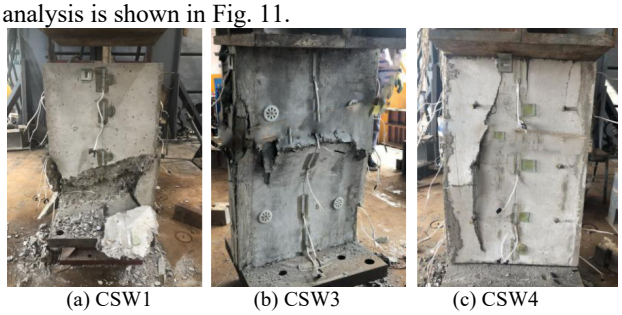

(a) CSW1 (b) CSW3 (c) CSW4

Fig. 11. Comparison chart of failure state.

4.2 Bearing capacity analysis

The test results of the ultimate axial load and the vertical displacement of each specimen are shown in Table 4. The ultimate load value of specimen CSW2 was small, standing at 69 % of the ultimate load of CSW1 specimen (the cast-in-place reinforced concrete shear wall). Except that Specimen CSW2 stops loading because the outer precast template was separated. The ultimate load values of the rest laminated shear wall specimens reached more than 80 % of specimen CSW1. For composite shear walls without any thermal insulation material, the bearing capacity of the specimens CSW3 with studs and CSW4 with CFRP shear connectors at the interface was 26 % and 22 % higher than specimen CSW2 with only ribs, respectively. For composite shear walls with thermal insulation materials, the bearing capacity of specimen CSW6 with ribs and bolts at the interface and specimen CSW7 with ribs and CFRP shear connectors were 11 % and 38 % higher than specimen CSW5 with only ribs, respectively. It is not uneasy to conclude that the bolts or CFRP shear connectors at the interface can effectively improve the ultimate load of the composite shear wall. The CFRP shear connector showed more improvement.

4.3 Load-displacement curve analysis

As shown in Fig. 12, the vertical displacement of each specimen was approximately linear with the load. The slope of the load-vertical displacement curve of the composite shear wall specimen with insulation layer was greater than the those without insulation materials. This is mainly because the prefabricated cement insulation composite plate of the composite shear wall with insulation material is well bonded with the wall core concrete in the loading process, which increases the effective thickness of the wall, thereby improving the vertical compression stiffness of the wall.

Table. 4. Test result.

Test specimen number	Ultimate load F_u (kN)	Vertical displacement D_u (mm)	Vertical compression stiffness $K_V = F_u / D_u$	Failure state
CSW1	1781.56	2.73	625.59	Axial compression failure
CSW2	1228.83	1.80	682.68	Failure of composite surface
CSW3	1551.52	2.15	721.64	Axial compression failure
CSW4	1497.91	2.38	629.37	Axial compression failure
CSW5	1425.59	1.32	1079.99	Axial compression failure
CSW6	1575.34	1.67	943.32	Axial compression failure
CSW7	1974.37	2.86	690.34	Axial compression failure

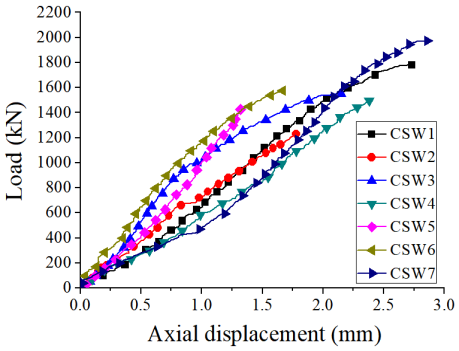

Fig. 12. Load-vertical displacement curve of each specimen.

Comparing the load-vertical displacement curves of each specimen, the load-vertical displacement curves of the specimens CSW4 and CSW7 with CFRP shear connectors on the interface were the closer to the full cast-in-place specimen CSW1, which indicates that the setting of CFRP shear connectors on the interface of the composite shear wall improves the performance of the composite shear wall.

As seen from Fig. 13(a), the lateral displacement of the upper part of the specimen CSW1 wall was significantly greater than the lower part, and the lateral displacement of the wall increased along the wall height direction. During the loading process, the lateral displacement of each measuring point of Specimen CSW1 increases uniformly, mainly because specimen CSW1 is a fully cast-in-place reinforced concrete shear wall with good integrity. As seen from Fig. 13(b), the interface bonding performance between the core concrete and the precast cement plate of specimen CSW2 with ribs only at the interface was weak. The precast cement plate sloughed during the loading process, resulting in an uneven stress and irregular lateral deformation of the specimen. It can be seen from Figs. 13(c) and 13(d) that the variation of lateral displacement of specimens CSW6 and CSW7 with studs or CFRP shear connectors at the interface was very close to specimen CSW1. The lateral displacement of the upper part is greater than that of the lower part of the wall. The lateral displacement of each measuring point increased uniformly with load. When the ultimate load was reached, the lateral displacement of each measuring point increased abruptly, indicating that the setting of studs or CFRP shear connectors at the interface can improve the bonding performance.

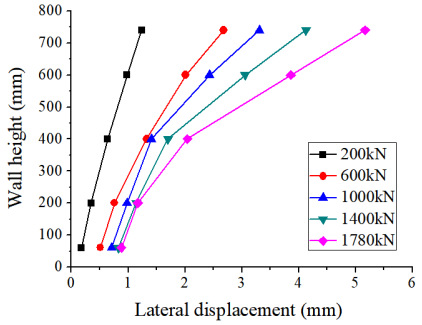

(a) CSW1

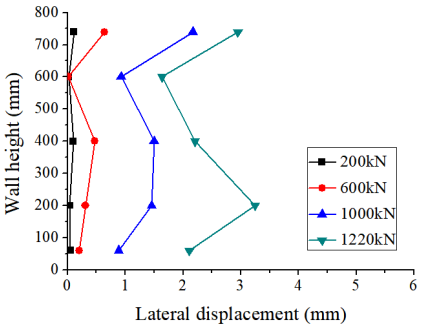

(b) CSW2

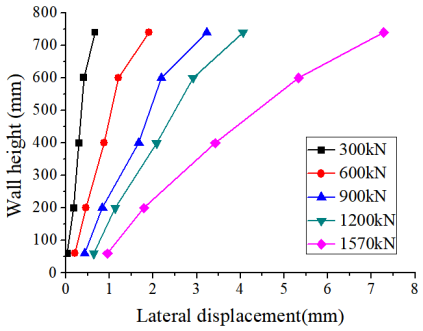

(c) CSW6

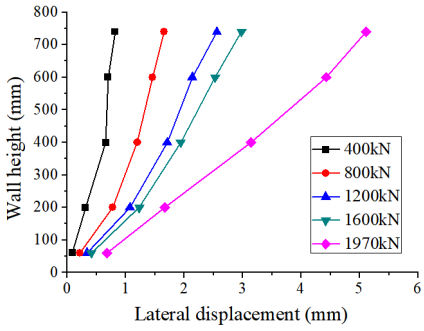

(d) CSW7

Fig. 13. Lateral displacement of specimen along wall height under different loads.

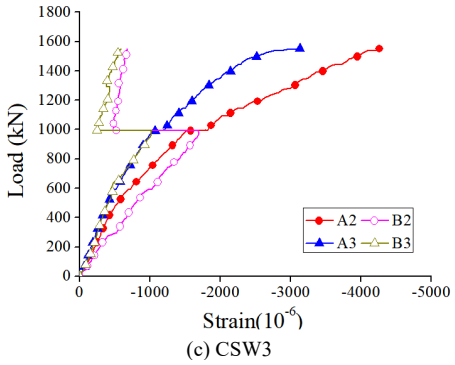

(c) CSW3

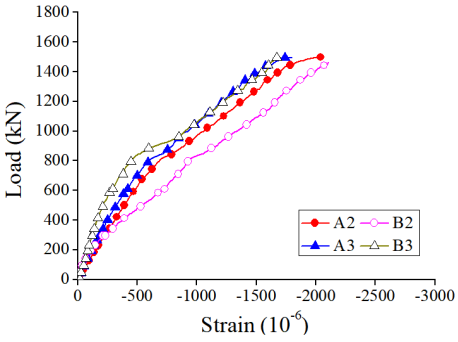

(d) CSW4

Fig. 14. Load-strain curve comparison between steel bar and concrete.

4.4 Load-strain curve analysis

Fig. 14 is the strain change chart of reinforcement strain measuring points A2, A3 and concrete strain measuring points B2, B3 located at 200 mm from the top and at 1/2 of the wall height.

As seen from Fig. 14(a), the strain variation of the reinforcement strain measuring point of specimen CSW1 was similar to the concrete strain measuring point at the corresponding position. The load-strain curve was basically coincident, which is mainly because the cast-in-place reinforced concrete shear wall structure has uniform stress and good integrity.

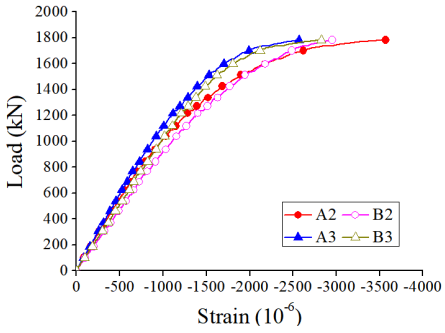

(a) CSW1

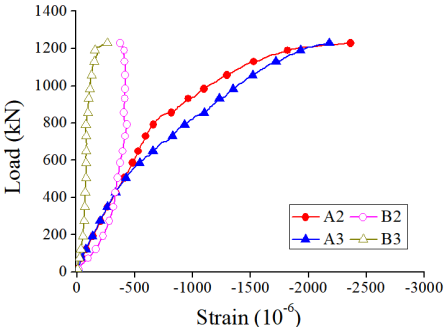

(b) CSW2

As seen from Fig. 14(b), the strain values of steel bar and concrete for CSW2 specimens were quite different. The reason is that the bond between prefabricated cement plate and core concrete is poor. The prefabricated cement plate gradually separated from the core concrete during loading and no longer beared synergistic forces. The strain values of the prefabricated formwork remained unchanged. The reinforcement in the core concrete continues to bear the load and the strain value increases with the increase of the load.

As seen from Fig. 14(c), in the early stage of loading, the strain of concrete and steel bars of specimen CSW3 with ribs and bolts at the interface increased linearly. The strains of steel bars were approximately equal to the strain value of the prefabricated cement plate at the corresponding positions. At the later stage of loading, the strain of the prefabricated cement plate changed abruptly, indicating that the prefabricated cement plate was well bonded with the wall core concrete in the early stage of loading, and that the wall core concrete and the prefabricated cement plates on both sides were well coordinated. The cracks in the joint between the prefabricated cement plate and the wall core concrete expanded and extended, resulting in a sudden change in the strain value of the prefabricated cement plate and no longer synchronize with the strain of the steel bar.

As seen from Fig. 14(d), the strain values of the steel bar and the precast concrete plate of specimen CSW4 changed synchronously in the loading process, showing good overall working performance and indicating the role of CFRP shear connectors for enhancing the bonding performance. The precast concrete plate and the wall core concrete can therefore work together well.

4.5 Calculation of axial compression bearing capacity

According to the Chinese Code for Design of Concrete Structures (GB50010-2010), the calculation of bearing capacity of reinforced concrete axial compression members should be consistent with:

$$N \leqslant 0.9\varphi(f_c A + f'_y A'_s) \quad (1)$$

where N is the axial pressure design value. φ is the stability coefficient of reinforced concrete members, which is related to the height-thickness ratio of the specimen and is valued according to the specification. f_c is the design value of axial compressive strength of concrete. A is the cross-sectional area of the component, when the reinforcement ratio of longitudinal ordinary steel bars is greater than 3 %, (A-A's) should be replaced. A_s' is the cross-sectional area of all longitudinal ordinary steel bars. f_y' is the design value of steel bar compressive strength.

According to the American norms (ACI 318-11), the axial compression bearing capacity of non-prestressed members with reinforcement is:

$$P_u = 0.8\varphi[0.85f_c'(A - A_{st}) + f_y A_{st}] \tag{2}$$

where ϕ is the resistance reduction coefficient of the structure, which is given as 0.85 for ordinary reinforced concrete axial compression members. f_c' is the standard value of compressive strength of the concrete cylinder. A is the cross-sectional area of the component. A_{st} is the sectional area of all longitudinal ordinary reinforcement. f_y is the standard value of the steel bar compressive strength.

According to the British code (BS8110-1), the bearing capacity of reinforced concrete members under axial compression is:

$$P_u = \frac{A_{st} f_y}{\gamma_s} + \frac{0.675 f_{cuk} A_c}{\gamma_c} \tag{3}$$

where A_{st} is the sectional area of all longitudinal ordinary reinforcement. f_y is the standard value of the compressive strength of the steel bar. γ_s is the partial coefficient of steel material, taken as 1.10. f_{cuk} is the standard value of compressive strength of the concrete cube with side length of 150 mm. A_c is the cross-sectional area of concrete. γ_c is the partial coefficient of concrete material, taken as 1.50.

Oberlender & Eerard conducted axial and eccentric compression tests on 54 composite shear wall specimens [22]. They proposed the calculation of axial compression bearing capacity of composite shear wall as:

$$P_u = 0.6 f_c' A\left[1 - \left(\frac{kH}{30T}\right)^2\right] \tag{4}$$

where f_c' is the standard value of compressive strength of the concrete cylinder. A is the cross-sectional area of the component. k is the structural coefficient, which is taken as 0.8 when both ends of the wall are consolidated and 1.0 when hinged. H is the height of the wall, and T is the wall thickness.

Benayoune et al. carried out axial compression and eccentric compression tests on six composite shear wall specimens [23]. Combined with the results of the finite element analysis, the calculation of axial compression bearing capacity of such composite shear wall was proposed as follows:

$$P_u = 0.4 f_c' A\left[1 - \left(\frac{kH}{40T}\right)^2\right] + 0.67 f_y A_{st} \tag{5}$$

where f_c' is the standard value of compressive strength of concrete cylinder. A is the cross-sectional area of the component. k is the structural coefficient, which is taken as 0.8 when both ends of the wall are consolidated and 1.0 when hinged. H is the height of the wall. T is the wall thickness. A_{st} is the sectional area of all longitudinal ordinary reinforcement. f_y is the standard value of steel bar compressive strength.

The size and material parameters of the seven shear wall specimens in this work were substituted into the Eqs. (1) to (5) to calculate the theoretical limit values. When the theoretical calculation was carried out, the concrete strength in each specification formula and the compressive strength of the steel bar were measured. The yield strength of the steel bar was measured also. The formula did not consider the material reduction partial coefficient and the resistance reduction coefficient. It is assumed that there is no bond and slip between the precast template and the concrete, and the interface bonding is good. The precast part and the cast-in-place part can bear the force together. The theoretical limit values calculated by each formula and the comparison with the experimental values are shown in Table 5.

It can be seen from Table 5 that the calculated limit values were mostly greater than the experimental values, which is unsafe in practical engineering applications. Comparing the calculated values from each formula, the axial compression bearing capacity calculated from the Chinese standard formula was closed to the experimental value. Therefore, the calculation formula of axial bearing capacity in Chinese standard is considered to be modified in this study to establish the calculation of axial compression bearing capacity suitable for the proposed new composite shear walls.

Table 5. Theoretical limit values of national standard and comparison with test values (kN).

Specimen number	Test value F	Chinese norms		American norms		British norms		Oberlender et al.		Benayoune et al.	
		N	$\frac{N}{F}$	P_{ACI}	$\frac{P_{ACI}}{F}$	P_E	$\frac{P_E}{F}$	P_O	$\frac{P_O}{F}$	P_B	$\frac{P_B}{F}$
CSW1	1782	1566	0.88	1371	0.77	1703	0.96	1777	1.00	1915	1.07
CSW2	1229	1601	1.30	1424	1.16	1768	1.44	1852	1.51	1990	1.62
CSW3	1552	1601	1.03	1424	0.92	1768	1.14	1852	1.19	1990	1.28
CSW4	1498	1601	1.07	1424	0.95	1768	1.18	1852	1.24	1990	1.33
CSW5	1426	1855	1.30	1658	1.16	2058	1.44	2203	1.54	2339	1.64
CSW6	1575	1855	1.18	1658	1.05	2058	1.31	2203	1.40	2339	1.49
CSW7	1974	1855	0.94	1658	0.84	2058	1.04	2203	1.12	2339	1.18

Since there must be bond slip between the precast formwork and the wall core concrete, it is inaccurate to think that the precast cement plate and the wall core concrete can be fully loaded together. The connection mode of the interface between the precast formwork and the wall core concrete has a great impact on the overall working

performance of the composite shear wall. Effective interface connection can significantly enhance the bonding performance and make precast formwork and wall core concrete work and sustain load together. Therefore, this study introduces the influence coefficient of interface connection mode, and establishes the calculation of axial compression bearing capacity of such new composite shear wall:

$$N = 0.9(f_c A_c + \lambda f_{c1} A_1 + \beta f_{c2} A_2 + A_s f_y) \quad (6)$$

where φ is the stability coefficient of reinforced concrete members, which is related to the height-thickness ratio of the specimen and is valued according to the Chinese specification. f_c is the axial compressive strength of the wall core concrete. A_c is the cross-sectional area of the wall core concrete. f_{c1} is the axial compressive strength of the precast concrete plate. A_1 is the section area of the precast cement plate. f_{c2} is axial compressive strength of the cement concrete in composite cement insulation composite plate. A_2 is the cross-sectional area of the cement board in composite cement insulation composite plate. λ is the influence coefficient of the interface connection mode on the bond between the precast concrete plate and wall core concrete. λ=0.6 is taken when using rib stud connection, λ=0.5 is taken when using rib CFRP shear connector, and λ=0 is taken when only using rib connection. β is the influence coefficient of the interface connection mode on the bond between precast cement insulation composite plate and wall core concrete. When using rib-reinforced CFRP shear connector, β=1 is taken, and β=0 at the case of rib-reinforced CFRP shear connector. A_s is the cross-sectional area of all longitudinal ordinary steel bars. f_y is the standard value of the compressive strength of the steel bar.

The calculated values of axial compression bearing capacity of each composite shear wall from Eq. 6 are shown in Table 6 and compared with the experimental values. The calculated values are in good agreement with the experimental values. In addition to specimen CSW2, the calculated values of the specimen were less than the experimental values, but the error is less than 12 %, which has a reasonable safety reserve. The calculated value of Specimen CSW2 was larger than the experimental value because the wall core concrete part of specimen CSW2 did not experience the axial compression failure. When the precast cement plates on both sides were separated, the specimen was considered to be damaged, so the experimental value was small.

Table. 6. Calculated value and comparison with test value.

Test specimen number	Test value (kN)	Calculated value (kN)	Calculated value/Test value
CSW1	1781.56	1565.94	0.88
CSW2	1228.83	1330.05	1.08
CSW3	1551.52	1492.75	0.96
CSW4	1497.91	1465.63	0.98
CSW5	1425.59	1330.05	0.93
CSW6	1575.34	1529.34	0.97
CSW7	1974.37	1786.95	0.91

5. Conclusions

To study the axial compression performance of a new-type of semi-prefabricated composite shear wall, six composite shear wall specimens and one cast-in-place shear wall specimen were prepared and subjected to the axial compression test. The failure state, bearing capacity, deformation and mechanical performance of each specimen were analyzed. The calculation of axial compression bearing capacity of this new-type composite shear wall was established. The main conclusions were obtained as following:

The failure modes of the composite shear wall were mainly divided into two types: the failure on the bonding surface and the failure of the axial compression. The specimens with only ribs at the interface were subjected to the failure of the composite surface, while the specimen with ribs and studs or ribs and CFRP shear connectors at the interface is subject to the failure of the axial compression similar to the cast-in-place shear wall due to the good bonding between the precast cement plate and the wall core concrete. Compared with setting ribs at the interface, setting rib studs or rib CFRP shear connectors at the interface can significantly improve the axial compression bearing capacity of the composite shear wall.

The deformation of the composite shear wall specimens with ribbed studs or ribbed CFRP shear connectors at the interface was the closest to the full cast-in-place shear wall specimens. The ribbed studs or ribbed CFRP shear connectors at the interface can effectively improve the bonding performance and to effectively improve the working performance of the composite wall. The reinforcement strain and concrete strain of specimens with ribbed CFRP shear connectors at the interface can change synchronously, showing good mechanical properties. The ribbed CFRP shear connectors at the interface have the most obvious improved bonding performance of precast cement plate and wall core concrete.

By revising the bearing capacity calculation of axial compression members in Chinese norms and introducing the influence coefficient of interface connection mode on the bonding performance of precast formwork and wall core concrete, the bearing capacity calculation of axial compression of this new-type semi-prefabricated composite shear wall was established. The calculated values were in good agreement with the experimental values, which can provide design reference for the practical engineering application.

The axial compression performance of the new-type composite shear wall structure was studied through experiments. The influence of ribs, studs and CFRP shear connector at the interface on the axial compression performance of this new-type composite shear wall were analyzed. The calculation formula of the axial compression bearing capacity of this new-type composite shear wall was established, which laid the foundation for the further study for the proposed composite shear wall. However, since the seismic fortification of building structures is extremely important, before promoting such new composite shear wall

structure system in China, it is necessary to study its seismic performance.

Acknowledgements

This work was supported by National Natural Science Foundation of China (52004010), and the Excellent Research Team of North China University of Technology (107051360021XN083/019).

References

1. Ye, M., Jiang, J., Chen, H. M., Zhou, H. Y., Song, D. D., "Seismic behavior of an innovative hybrid beam-column connection for precast concrete structures". *Engineering Structures*, 227, 2021, pp. 111436.
2. Kataoka, M. N., Ferreira, M. A., Homce de Cresce El Debs, Ana Lucia., "Nonlinear FE analysis of slab-beam-column connection in precast concrete structures". *Engineering Structures*, 143, 2017, pp. 306-315.
3. Wang, S. R., Wu, X. G., Yang, J. H., Zhu, S., "Acoustic emission characteristics and dynamic damage constitutive relation of shale ceramsite concrete subjected to loading tests". *Journal of Materials in Civil Engineering*, 32(8), 2020, pp. 04020202.
4. Wu, X. G.,Wang, S. R.,Yang, J. H., Zhao, J. Q., Chang, X., "Damage characteristics and constitutive model of lightweight shale ceramsite concrete under static-dynamic loading". *Engineering Fracture Mechanics*, 258, 2021, pp. 108137.
5. Arthi, S., Jaya, K. P., "Seismic performance of precast shear wall-diaphragm connection: a comparative study with monolithic connection". *International Journal of Civil Engineering*, 18(4), 2019, pp. 9-17.
6. Benayoune, A., Samad, A. A. A., Trikha D. N., Ali, A. A. A., Ellinna, S. H. M., "Flexural behavior of precast concrete sandwich composite panel-Experimental and theoretical investigations". *Construction and Building Materials*, 22(4), 2008, pp. 580-592.
7. Benayoune, A., Samad, A. A. A., Trikha, D. N., Ali, A. A. A., Ashrabov, A. A., "Structural behavior of eccentrically loaded precast sandwich panels". *Construction and Building Materials*, 20, 2006, pp. 713-724.
8. Frankl, B. A., Lucier, G. W., Hassan, T. K., Rizkalla, S. H., "Behavior of precast, prestressed concrete sandwich wall panels reinforced with CFRP shear grid". *Pci Journal*, 56(2), 2011, pp. 42-54.
9. Tomlinson, D., Fam, A. "Experimental investigation of precast concrete insulated sandwich panels with glass fiber-reinforced polymer shear connectors". ACI Structural Journal, 111(3), 2014, pp. 595-605.
10. Bei, C., Yuan, C., Daniel, T. W. L., "Experiment and numerical study of a new bolted steel plate horizontal joints for precast concrete shear wall structures". *Structures*, 32, 2021, pp. 760-777.
11. Mohamad, N., Omar, W., Abdullah, R., "Precast lightweight foamed concrete sandwich panel (PLFP) tested under axial load: preliminary results". *Advanced Materials Research*, 250-253, 2011, pp. 1153-1164.
12. Ahmad, I., Goh, W. I., Samsuddin, S., Mohamad, N., Rahman, M. H. A., Samad, A. A. A., "Structural behaviour of precast lightweight foamed concrete sandwich panel (PLFP) with double shear truss connectors under axial load: preliminary result". *Advanced Materials Research*, 795, 2013, pp. 414-418.
13. Ye, Y. H., Xue, Z. H., Sun, Y., Wang, H., "Experimental study on seismic precast NC composite behavior of SCC and shear wall". *Journal of Building Structures*, 7, 2014, pp. 138-144.
14. Wang, M. F., Zou, T. Q., "Experimental Study on seismic behavior of precast composite shear wall with concealed bracing". Journal of Hunan University (Natural Sciences), 1, 2017, pp. 54-64.
15. Zhang, X. G., Wang, S. R., Gao, X., He, Y. S., "Seismic behavior analysis of recycled aggregate concrete-filled steel tube column". *Journal of Engineering Science and Technology Review*, 12(4), 2019, pp. 129-135.
16. Chu, M. J., Liu, J. L., Hou, J. Q., Liu, M. H., Wang, G., Qiu, G. M., "Experimental study on mechanical behavior of superimpose slab shear walls without interface steel". *Journal of Building Structures*, 10, 2016, pp. 90-97.
17. Song, X. R, Liu, P. G., Zhao, D. F., Qu, Y. T., Zhang, X. Y., "Study on stay-in-place cement formwork and the application". *Advanced Materials Research*, 163-167, 2011, pp. 952-955.
18. Zhang, X. G., Kuang, X. M., Wang, F., Wang, S. R., "Strength indices and conversion relations for basalt fiber-reinforced recycled aggregate concrete". *DYNA*, 94(1), 2019, pp. 82-87.
19.Wang, S. R., Zhao, J. Q., Wu, X. G., Yang, J. H., Liu, A., "Meso-scale simulations of lightweight aggregate concrete under impact loading". *International Journal of Simulation Modelling*, 20(2), 2021, pp. 291-302.
20. Drapaluk, M., "Influence of reinforced concrete forming features on mechanical characteristics". *Technical Journal*, 13(2), 2019, pp. 86-91.
21. Song, X. R., Qu, Y. T., Zhang, X. Y., Niu, W., Jiang, Y. F., "Design and analysis of the support system for cement-base formwork". *Advanced Materials Research*, 374-377, 2011, pp. 1249-1253.
22. Oberlender, G. D., Eerard, N. J., "Investigation of reinforced concrete walls". *Journal Proceedings*, 74(4), 1977, pp. 256-263.
23. Benayoune, A., Samad, A. A. A., Ali, A. A. A., Trikha, D. N., "Response of precast reinforced composite sandwich panels to axial loading". *Construction and Building Materials*, 21(3), 2007, pp. 677-685.